2014 IEEE International Conference on Robotics & Automation (ICRA)
Hong Kong Convention and Exhibition Center
May 31 - June 7, 2014. Hong Kong, China

A novel robust template matching method to track and follow body targets for NIUTS

Norihiro Koizumi, Takakazu Funamoto, Joonho Seo, Dongjung Lee, Hiroyuki Tsukihara, Akira Nomiya, Takashi Azuma, Kiyoshi Yoshinaka, Naohiko Sugita, Yukio Homma, Yoichiro Matsumoto, and Mamoru Mitsuishi

***Abstract*— The authors have developed a bed-type non-invasive ultrasound theragnostic system (NIUTS) that compensates for movement by tracking and following the area to be treated by stereo ultrasound imaging while irradiating high-intensity focused ultrasound (HIFU) onto the affected area. In this paper, we propose a novel robust template matching method to track and follow body targets, which include tumors and stones for the NIUTS. The proposed novel robust template matching method could be applied to a motion tracking of the real human kidney based on the ultrasound images, which is the first successful report as far as I know. This robust visual servoing method could be a great tool to treat the tumors and stones precisely and safely.**

I. INTRODUCTION

Recently, research and development related to robot vision technology, such as visual servoing and image guidance technologies, has increased in various fields [1]-[4]. Among those technologies, medical applications are very promising.

In the field of open surgeries [5]-[6], Nakamura et al. proposed synchronizing a master-slave type surgical system with organ movement by using a 955-fps optical high-speed CCD camera. The system, called a "motion canceller system," consists of a master-slave system, a visual stabilization system, and a motion stabilization system [5].

However, such an optical high-speed camera cannot be applied to our proposed non-invasive therapeutic and diagnostic (theragnostic) system because skin and other healthy tissues cannot be injured.

Among the applications in the field of radio surgeries [7]-[10], Cyber Synchrony®, which is a CyberKnife® real-time image-guided system, uses externally placed optical markers on a patient's skin for target detection and motion compensation. Li, et.al., developed an algorithm for realtime volumetric image reconstruction and 3D tumor localization based on a single x-ray projection image for lung cancer radiotherapy [10].

Several visual servoing methods for ultrasound imaging have been introduced [11]-[14]. Abolmaesumi et al. developed a robot-assisted ultrasound diagnostic system with a visual servo controller. In this system, an operator, a robot controller, and an ultrasound image processor have shared control over the motion of the robot positioning the ultrasound transducer[11].

N. Koizumi, T. Funamoto, J. Seo, D. Lee, T. Azuma, N. Sugita, Y. Matsumoto, and M. Mitsuishi are with the School of Engineering, University of Tokyo, Hongo, Bunkyo-ku, Tokyo 113-8656, Japan (e-mail: nkoizumi@nml.t.u-tokyo.ac.jp). H.Tsukihara, A.Nomiya, and Y.Homma are with the School of Medicine, the University of Tokyo, 7-3-1 Hongo, Bunkyo-ku, Tokyo 113-8656, Japan. K.Yoshinaka is with the Advanced Industrial Science and Technology (AIST), 1-2-1 Namiki, Tsukuba, Ibaraki 305-8564 Japan.

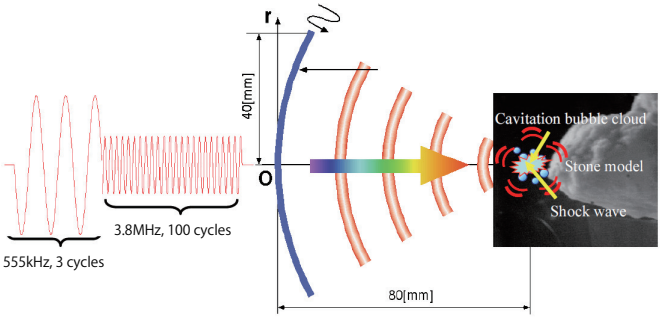

Fig. 1. Destruction of a model kidney stone by High Intensity Focused Ultrasound (HIFU).

Ivana et al. propose a method for off-line segmentation and tracking of cardiac structures in ultrasound image by utilizing contour information of the organ [12]. However, the realtime performance is not enough to be applied to our system.

Ultrasound speckles of the target can be directly used for motion tracking. Tracking based only on the consistency of the speckle pattern in a single ultrasound image is error-prone and unreliable due to the elevational separation (out-of-plane motion) of the target.

Speckle decorrelation change can be used to estimate out-of-plane motion with a single ultrasound plane [13]. So far, studies are available only in fully developed ultrasound images, which require precalibration of the speckle decorrelation curve for materials similar to the target material.

In High Intensity Focused Ultrasound (HIFU) therapy (Fig. 1), ultrasound beams are generated and focused on a small region by spherical transducers. The HIFU focus is smaller than that of the conventional treatment methods, such as Extracorporeal Sock Wave Lithotripsy (ESWL) [15].

Thus, it becomes possible to concentrate the energy on a small region in the body to treat the affected area, such as tumors and stones, in the focal volume without damaging surrounding or overlying healthy tissues [16].

Using non-invasive HIFU is an attractive and promising alternative to current open and endoscopic surgeries so as to reduce the load of patients and medical professionals. The JC Haifu®system [17] and ExAblate®system [18] are widely known and used in clinical practice [19][20].

A total of 40,000 clinical cases have been treated in variety of tumors [21][22], i.e, uterine fibroids, osteosarcoma, liver, kidney, pancreas, and breast cancers, fibroid tumors, tumor symptoms, soft tissue and metastatic cancers, etc.

However, there was no compensation for the movement of the affected area in the organs, which is caused by respiration, heartbeat, etc. Preventing such movement while irradiating an affected area with focused ultrasound is generally difficult for both the medical professional and the patient.

We herein propose an non-invasive ultrasound theragnostic system (NIUTS) that compensates for movement by tracking and following the area to be treated by stereo ultrasound imaging while irradiating the affected area with HIFU. Here, theragnostics is an compound word composed of therapeutics and diagnostics.

The proposed system uses focused ultrasound to destroy tumors and stones without damaging healthy tissue. This is achieved by tracking and following the affected area (kidney stones / tumors, in the present study) precisely and robustly in order to compensate for movement due to the patient's respiration, heartbeat, and other causes.

The overall goal of this research project is to enhance the servo performance based on our original medical support system construction methodology, which is called "technologizing and digitalizing medical professional skills (TDMPS)," and our accumulated unique core technologies [23][24].

In this paper, the concept of a NIUTS is first described. Second, we clarify the functional requirements for NIUTS and illustrate an implemented bed-type NIUTS. Third, we discuss the required servoing precision and the problems and solutions associated with visual servoing of target tumors and stones in the body by using ultrasound images.

Fourth, a novel robust template matching method to track and follow the affected area is proposed to cope with the above-mentioned problems. Then, we conduct (i) offline tracking experiments and (ii) realtime online tracking and following experiments of the human kidney motion of a healthy subject to confirm the effectiveness of the proposed novel robust template matching method.

II. NON-INVASIVE ULTRASOUND THERAGNOSTIC SYSTEM

A. Concept of Non-invasive Ultrasound Theragnostic System

Based on recent studies, HIFU is regarded as very promising medical technology for the treatment of tumors and stones. However, the respiratory-induced motion of the kidney seriously decreases the efficacy of HIFU treatment.

To overcome this limitation, most treatment using HIFU has required the patient to be awake during the operation to control respiratory excursions in the kidney. As expected, patients and surgeons prefer to perform HIFU therapy under general anesthesia to ensure patient comfort and immobility. Accordingly, it is imperative to develop methods for respiratory motion compensation in the therapeutic HIFU system.

The concept of a non-invasive ultrasound theragnostic system is one that compensates for movement by tracking and following the affected area by stereo ultrasound imaging while irradiating the affected area with HIFU.

The proposed system uses focused ultrasound to destroy tumors and stones without damaging healthy tissues. This is achieved by tracking and following the affected area precisely and robustly to compensate for movement due to the patient's respiration and other causes.

B. Functional Requirements

Clarification of the functional requirements is important in order to realize efficient medical support systems. The specification of the structuring functional requirements, considering the system implementation for NIUTS, is shown in the reference [25].

In the present paper, we propose a novel robust template matching method to track and follow real body targets, which incorporate tumors / stones.

Here, it should be noted that the robust and precise motion canceling is one of the unmet medical needs to apply HIFU therapy, though which is strongly required to cancel the motion of the affected area in the body.

Therefore the medical professional cannot consider HIFU therapy as a first choice in the current HIFU systems for the moving affected area to be treated such as kidney stones / tumors, though HIFU has a great potential due to its non-invasiveness.

This novel robust template matching method could be a great tool, which is mainly related to the following functional requirements to apply HIFU therapy to the treatments of stones / tumors, which moves in accordance with the respiration / heartbeat.

(FR-1.2) Extracting the affected area.
(FR-1.4) Tracking and following the affected area.
(FR-1.5) Monitoring the affected area.

C. Implemented System Configuration

The bed-type NIUTS (Figs. 2) was constructed based on the structured functional requirements, as described in Section II-B. In Fig. 2(a), XYZ stage, which is configured in the water tank under the bed, moves the tip of the system (ultrasound probes and HIFU transducers).

Here, it should be noted that the XYZ stage is configured in the water aiming at the following two effects: (i) Secure the ultrasound paths to the affected area in the body through the water, silicon membrane, and body tissues, (ii) Reduce the load of the motor driver to move the tip of the system and absorb the unintentional mechanical oscillation (The verification of this effect is out of the scope of this paper and our future work).

A magnetic positioning sensor is attached to the human body in order to detect and cope with the active movements of the human body (The utilization of this sensor is out of the scope of this paper and our future work).

Stereo diagnostic images are acquired using two diagnostic probes. Here, HIFU Transducer hasn't been implemented yet in Fig. 2(b), because this is the prototype system and we have

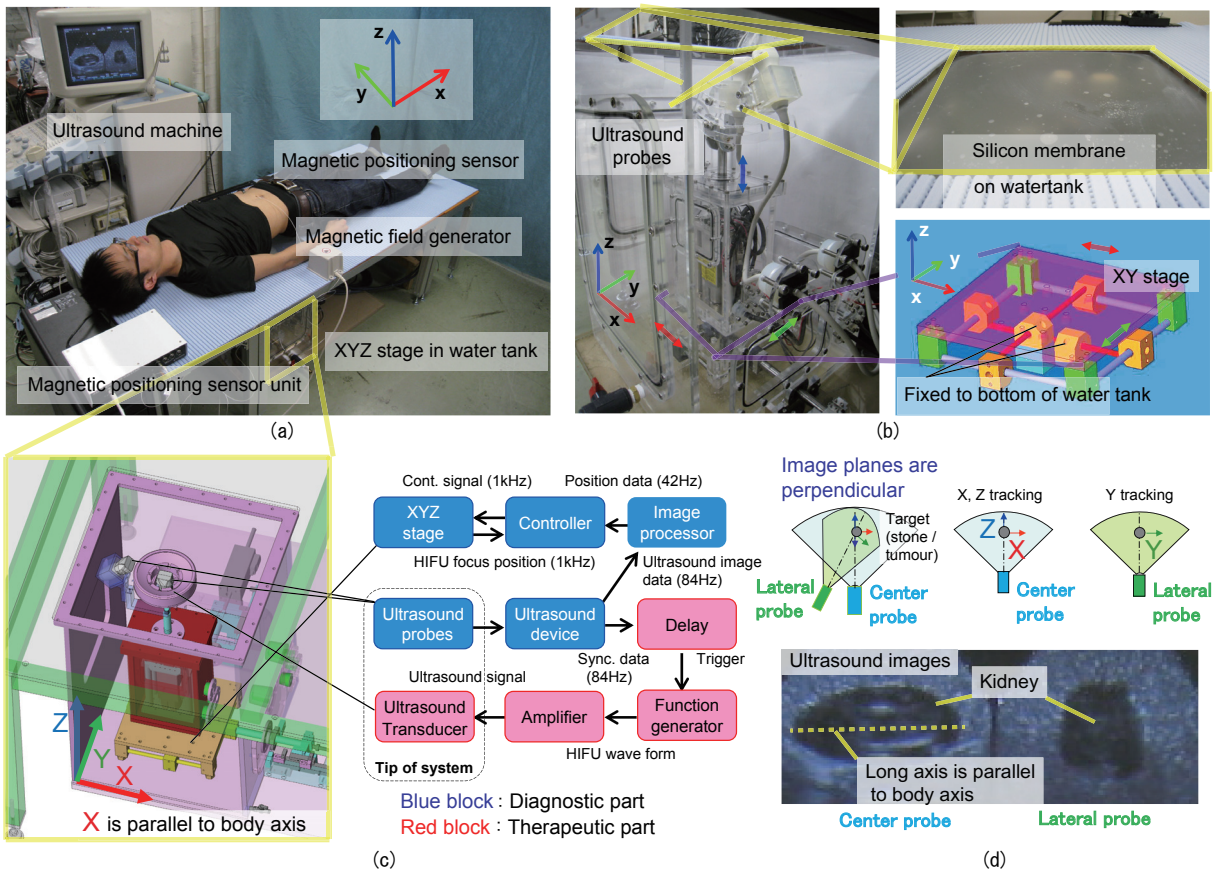

Fig. 2. System configuration of Non-Invasive Ultrasound Theragnostic System (NIUTS).

to avoid the possibility to injure the human body by HIFU transducer by accident.

These images are then used to determine the 3D positioning data of the affected area and the focus position of the HIFU. Here, the specification of the visual servoing method is described in Section II-D. In the control, the focus point tracks and follows the target kidney stone using the 3D positioning data [26]. The HIFU irradiates the kidney stone using a function generator, an amplifier, and a transducer. The HIFU irradiation parameters are given in Reference [16].

The robot has a spherical piezoelectric transducer and two ultrasound probes (Fig. 2(c)), one of which is located in the center of the piezoelectric transducer and the other of which is located on the lateral side of the piezoelectric transducer. These two probes satisfy the following two requirements:

(i) The image planes of the probes are mutually perpendicular (Fig. 2(d)).

(ii) The focus of the HIFU, which is irradiated by piezoelectric transducers, is located on the image planes of both probes (Fig. 2(d)).

The two ultrasound image planes are shown in Fig. 2(d). The ultrasound image on the left is acquired by the probe in the center of the piezoelectric transducer, and the ultrasound image on the right is acquired by the probe on the lateral side of the piezoelectric transducer. The real human kidney is located in those ultrasound images. In the image of the center probe, the long axis of the kidney, which is parallel to the body axis, is confirmed. The sectional image of the kidney, which is perpendicular to the long axis, is confirmed in the image of the lateral probe.

D. Basic Visual Servoing Method

Ultrasound images of the kidney have high intensity characteristic patterns in the kidney. We apply a template matching method by utilizing these patterns, as our basic visual servoing method. Template matching is one of the strong techniques for visual servoing to find parts of an image in the realtime input image (search image), which match a pre-obtained template model image.

Here, contact status, between the ultrasound probes and the skin surfaces, have significant influence on the intensity of the ultrasound image, e.g., the center of the ultrasound image is brighter than the side. To eliminate this effect, we apply the normalized correlation coefficient as an indicator of similarity, which is defined as the following equations.

$$R^{u,v} = \frac{\sum_m^M \sum_n^N (F^{u,v}(m,n) - \bar{F}^{u,v})(T(m,n) - \bar{T})}{\sqrt{\sum_m^M \sum_n^N (F^{u,v}(m,n) - \bar{F}^{u,v})^2} \sqrt{\sum_m^M \sum_n^N (T(m,n) - \bar{T})^2}} \quad (1)$$

$$\bar{F}^{u,v} = \frac{\sum_m^M \sum_n^N F^{u,v}(m,n)}{M \times N} \quad (2)$$

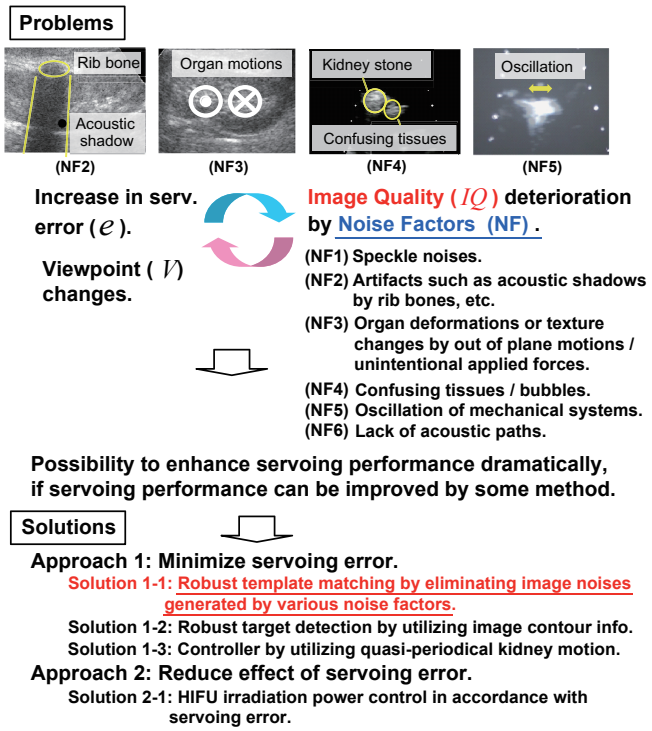

Fig. 3. Problems and solutions of visual servoing using ultrasound images.

$$\bar{T} = \frac{\Sigma_m^M \Sigma_n^N T(m,n)}{M \times N} \tag{3}$$

Here, $T(m,n)(M \times N)$: Template model, $F(x,y)$: Search image, $F^{u,v}(m,n)$: Partial image, which have the same size as the template model and have the starting point of (u,v) in the search image $(F^{u,v}(m,n) = F(u+m, v+n))$.

It is important to select the effective templates for the effective visual servoing by template matching methods. Templates, which are fit for visual servoing, have generally these 2 characteristics: (i) Templates include many characteristic patterns. (ii) Image patterns don't fluctuate so much, between the templates and the corresponding realtime input images.

Noise factors, which change the image patterns, are shown in Section II-F. To cope with this problem, we have to develop the novel robust visual servoing method for body targets, which is illustrated in Section III.

E. Required Servoing Precision

In this section, we discuss the required servoing precision of our special theragnostic system. In our research project, both stones and tumors are our targets to track and follow. In the case of stones, the stone, whose diameter is under 4mm, is expelled out of the body naturally.

Therefore, it is required to track and follow the stone whose radius r_{stone} is 2mm at the minimum. The radius of the HIFU focus r_{focus} is approximately 0.5 mm. The HIFU irradiated lesion is ellipsoidal, with a long axis of approximately 10 mm and a short axis of approximately 1 mm in our system [16].

Therfore, the required target tracking precision E^d_{stone}, in order not to injure the healthy tissues, is introduced as the following relation, which is based on the advice of the medical professional.

$$E^d_{stone} \leq \min(r_{stone} - r_{focus}) = 2\text{mm} - 0.5\text{mm} = 1.5\text{mm} \tag{4}$$

Concerning the case of tumors, the expansion of the irradiation scope, to cancel the respiratory motion, is required to be set within 5mm in each three dimensional directions in the radiation therapy [27]. In our study, we set the half of the above-mentioned expansion of the irradiation scope as our required servoing precision E^d_{tumor} as shown in the next relation, which is based on the advice of the medical professional.

$$E^d_{tumor} \leq 2.5\text{mm} \tag{5}$$

Here, the resolution of the ultrasound diagnostic image is approximately 0.3 mm when a 3-MHz probe is applied.

F. Problems and Solutions Associated with Visual Motion Tracking by Ultrasound Images

In this section, we discuss the problems and solutions associated with visual motion tracking by ultrasound images. First, we discuss the problems in extracting, servoing, and monitoring the affected area.

As described in Fig. 3, the noise factors, which deteriorate the image quality (IQ, which could be evaluated by the correlation value between the realtime input ultrasound images and the template model, which is shown in Section II-D) are classified into the following seven factors: (NF1) speckle noises (random bright spots), (NF2) artifacts such as acoustic shadows generated by the high acoustic impedance tissues like rib bones. (NF3) organ deformations or texture pattern changes in the ultrasound images due to the out of plane organic motions [13] / the unintentional applied forces by the surrounding tissues, such as the pulses of the surrounding vessels, (NF4) confusing surrounding tissues or bubbles, which are generated by HIFU irradiation, image aliases, etc. (NF5) blur noise caused by oscillation of the mechanical systems, (NF6) Lack of the acoustic paths for the diagnostic ultrasound, which is caused by the unstable contact states, gases in the body.

Servoing errors cause the ultrasound images to change due to the change of the viewpoints of the ultrasound probes, which in turn increases the servoing error. This negative spiral causes the servoing performance to become increasingly worse.

However, if the servoing performance can be improved by some method that results in a positive spiral, the possibility of dramatically enhancing the servoing performance is increased.

To overcome the problems related to errors, we consider two approaches. The first approach is to minimize the servoing error. This approach attempts to enhance both the efficiency of the therapy and the safety of the patient. The

second approach is to reduce the effect of the servoing error. This approach primarily contributes to safety by not injuring healthy tissues surrounding the affected area.

With respect to the first approach, we developed two solutions to enhance not only the servoing performance to realize efficient therapy but also the safety of the patient [25][26]. One solution is robust detection of the target kidney stone position based on information in the ultrasound image [25]. The second solution is a controller that compensates for the periodic respiratory motion of the affected area [26].

In the present work, we propose a novel robust template matching method to track and follow the body targets, which incorporates the tumors and stones. With respect to the controller in the second approach, we developed a solution to control the HIFU irradiation power in accordance with the servoing error to enhance patient safety [25].

III. ROBUST TEMPLATE MATCHING METHOD TO TRACK AND FOLLOW BODY TARGETS

A. Concept of novel robust template matching method

The servoing error increases when the IQ for visual servoing of the target is decreased, as mentioned in Section II-F. The noise factors, which deteriorate the IQ, can be mainly classified as follows:

(NF1) Speckle noises (random bright spots).
(NF2) Artifacts such as acoustic shadows.
(NF3) Organ deformations or texture pattern changes.
(NF4) Confusing surrounding tissues or bubbles.
(NF5) Blur noise caused by mechanical oscillation.
(NF6) Lack of the acoustic paths.

The concept of our proposed robust template matching method is to exclude the regions where the image texture patterns change greatly during the quasi-periodical motion of the target kidney. It should be noted that the ultrasound images, having the same phase in each period, look similar. Likewise, Each of the above-mentioned noise factors tends to appear in the same phase in each period.

In this section, we introduce the following three steps to obtain a robust template.

[Step 1] Acquire kidney video images and the trajectory pre-operatively.
[Step 2] Eliminate image texture pattern changing regions due to acoustic shadows.
[Step 3] Eliminate regions of image texture pattern changing regions by noise factors besides acoustic shadows.

B. Step 1: Acquisition of Kidney Video Images Pre-operatively

In this step, we have the following three sub-steps.

[Step 1-1] Acquire kidney video images for S_t s (30 s is the default value in the present system). These images should empirically include at least three average periods ($3T_{avg}$) of repetitive respiratory motion ($S_t > 3T_{avg}$).
[Step 1-2] Acquire a trajectory of the kidney by applying template matching to the obtained video images (Fig. 4).

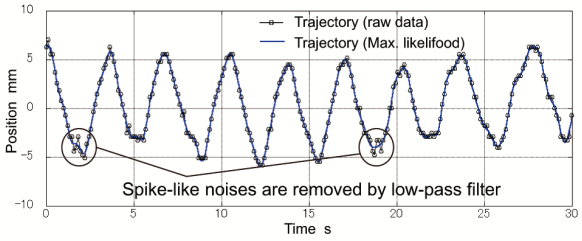

Fig. 4. Acquired raw trajectory [Step 1-2] and filtered kidney trajectory [Step 1-3].

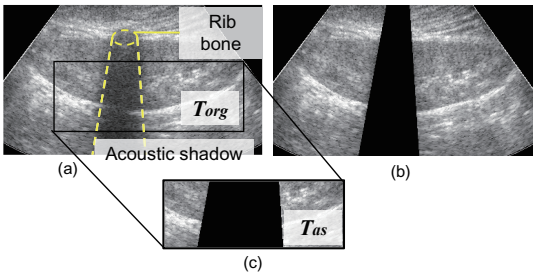

Fig. 5. Eliminating image pattern changing regions due to acoustic shadows. (a) Selecting original template T_{org} in the first frame of the video image obtained in Step 1-1. (b) Extracting acoustic shadow area. (c) Eliminating the acoustic shadow area from T_{org} by considering the motion area of the kidney in a period. We obtain the new template T_{as}.

[Step 1-3] Apply a low-pass filter (cut-off frequency is 3Hz in our system) to the obtained trajectory in the abovementioned [Step 1-2] and acquire the maximum likelihood trajectory (Fig. 4).

We obtain video images of the kidney motion and the maximum likelihood trajectory in this step. Fig. 4 shows that a continuous and smooth trajectory (we define this trajectory as the maximum likelihood trajectory) can be obtained by applying a low-pass filter to the original raw trajectory. The cut-off frequency is set 3Hz, because it is confirmed that the power over 1 Hz is under 1 percent of that of the main frequency (around 0.15 Hz) by FFT analysis of the respiratory motion.

C. Step 2: Eliminating Image Texture Pattern Changing Regions by Acoustic Shadows

If no acoustic shadow exists in the video images which are obtained in Step 1-1, skip this step and go to Step 3. If acoustic shadows exist, we perform the following three sub-steps to eliminate the image texture pattern changing regions by the acoustic shadows as Step 2.

[Step 2-1] Select the original template T_{org} in the first frame of the video image obtained in [Step 1] (Fig. 5(a)).
[Step 2-2] Extract the acoustic shadow area (Fig. 5(b)).
[Step 2-3] Eliminate the acoustic shadow area from T_{org} by considering the motion area of the kidney in a period. We obtain a new template T_{as} (Fig. 5(c)).

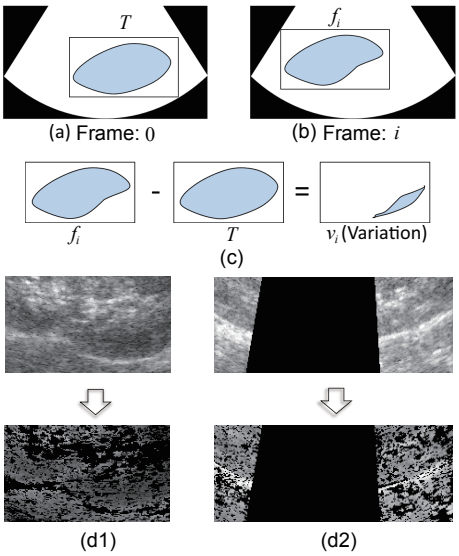

Fig. 6. Eliminating image texture pattern changing regions by noise factors besides acoustic shadows. Calculating the intensity difference between the original template (a) and the partial image f_i (b), which corresponds to template T in the i th frame. We obtain the image texture pattern change v_i (c). Eliminating the acoustic shadow area and the region whose image texture pattern change v_a is greater than the threshold value v_{th} from T. We obtain template T. Here, (d1) does not have an acoustic shadow, but (d2) does have an acoustic shadow.

D. Step 3: Eliminating Image Texture Pattern Changing Regions by Noise Factors Besides Acoustic Shadows

In this step, we perform the following three sub-steps.

[Step 3-1] Calculate the intensity difference between the original template T (Fig. 6(a)) and the partial image f_i (Fig. 6(b)), which corresponds to template T in the i th frame. We obtain the image texture pattern change v_i as the following equation (Fig. 5(c)).

$$f_i - T = v_i \quad (i \in \mathbb{N} = 1, 2, \cdots) \tag{6}$$

[Step 3-2] Calculate v_i for all frames ($i = 1, \cdots, \lfloor F_r \cdot S_t \rfloor$) and obtain the average image texture pattern change v_a. This shows the image texture pattern change during the quasi-periodical kidney motion. Here, F_r is the frame rate of the obtained video images in Step 1-1.

$$v_a = \frac{1}{\lfloor F_r \cdot S_t \rfloor} \Sigma_{i=1}^{\lfloor F_r \cdot S_t \rfloor} |v_i| \tag{7}$$

[Step 3-3] Eliminate the acoustic shadow area and the region whose image texture pattern change v_a is greater than the threshold value v_{th} from T. We obtain template T (Fig. 6(d1) and (d2)). Here, (d1) is the obtained T that does not include an acoustic shadow. On the other hand, the image in (d2) includes an acoustic shadow. The black region in (d1) and (d2) is eliminated from the template to calculate the correlation value between template T and the realtime input video images so as to enhance the robustness to track and follow the body targets, which incorporate stones and tumors.

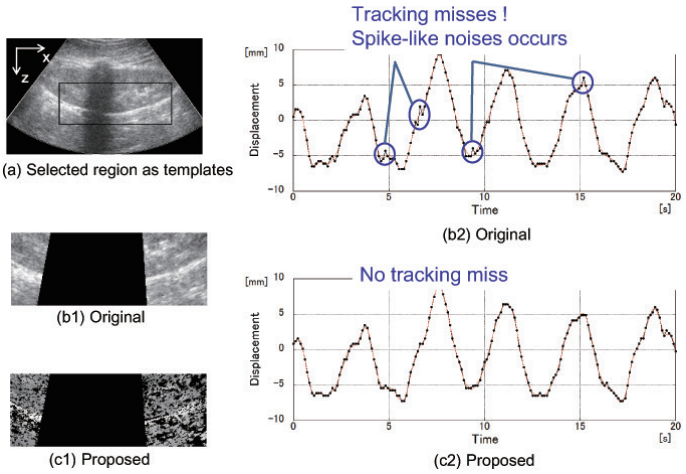

Fig. 7. Experimental results of offline motion tracking experiments of kidney by larger templates.

IV. EXPERIMENTS

We conducted (i) offline tracking experiments and (ii) realtime online tracking and following experiments of the human kidney motion of a healthy subject to confirm the effectiveness of the proposed robust template matching method. We compared the proposed method with the conventional and original template matching methods.

A. Offline Motion Tracking Experiments of Kidney by Larger Templates

We conducted experiments of offline tracking and following the target kidney to confirm the effectiveness of the proposed robust template matching method. In the present experiment, a larger template is selected. This template is larger than that in the following Section IV-B. The experimental results are shown in Fig. 7.

In the figure, as just mentioned, the larger region is selected as a template. Spike-like noises occur in the tracking by the conventional original template, whereas no tracking misses are observed in the tracking by the proposed robust template. However, the improvement of the tracking performance is relatively small as compared to that by the smaller templates in Section IV-B.

B. Offline Motion Tracking Experiments of Kidney by Smaller Templates

In this present experiment, the smaller template is selected, in contrast to the one selected in the above Section IV-A. The experimental results are shown in Fig. 8.

In the figure, the smaller region is selected as a template. Spike-like noises occur more frequently in the tracking by both the conventional original template and that by the experimental result described in Section IV-A.

The average tracking miss rate of the proposed robust template matching method is 4.5 percent, while that of the conventional original template is 15.6 percent in 30 randomly selected templates (Fig. 8). It is confirmed that the proposed

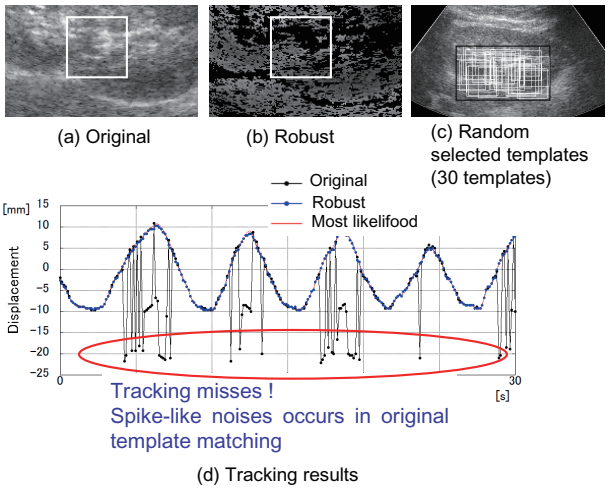

Fig. 8. Experimental results of offline motion tracking experiments of kidney by smaller templates.

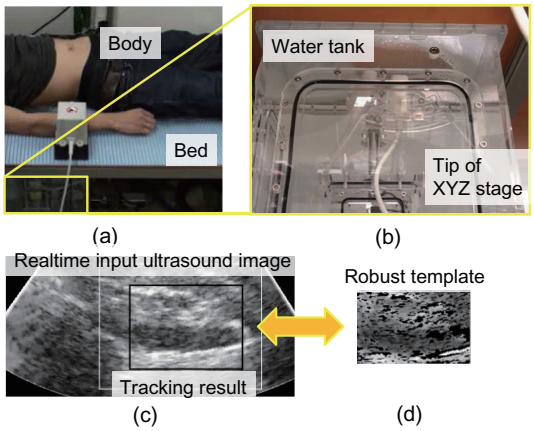

Fig. 9. Experimental environment of realtime tracking and following of kidney. (a) Human body and bed, (b) Water tank and tip of XYZ stage, (c) Real-time input ultrasound image and tracking result, (d) Proposed robust template.

template matching method is more effective when smaller templates are available.

C. Realtime Tracking and Following of kidney

We conducted experiments of realtime motion tracking and following the target human kidney to confirm the effectiveness of the proposed robust template matching method. The experimental environment is shown in Fig. 9.

The experimental results are shown in Figs. 10 and 11. We selected the template region to be as large as possible (Fig. 10(a1) and (b1)): (a1) shows the selected template of the original template matching method, and (b1) shows that of the proposed robust template matching method. The selected regions of the templates are almost the same for (a1) and (a2).

Fig. 10(a2) and (b2) shows the robot trajectory in the X and Z axes during tracking and following the target kidney: (a2) is the trajectory by the original template matching method, and (b2) is that by the proposed robust template matching method.

Fig. 10 shows that a tracking miss occurs with the original template matching method, whereas the proposed robust template matching method has almost no tracking miss. A smoother trajectory of the robot (x) can be acquired by the robust template matching method than by the original template matching method.

These results show that the tracking misses and errors by the original template matching method could be dramatically reduced by using the proposed robust template matching method. Therefore, the effectiveness of the proposed robust template matching method to track and follow the target kidney motion in real time is confirmed.

The smoothness is very important to secure the image quality (IQ), because oscillations generate blur noise and the tracking error makes the image quality worse, as described in Section II-F.

Fig. 11 shows the correlation value, between the ultrasound image and the template, a trajectory of the robotic

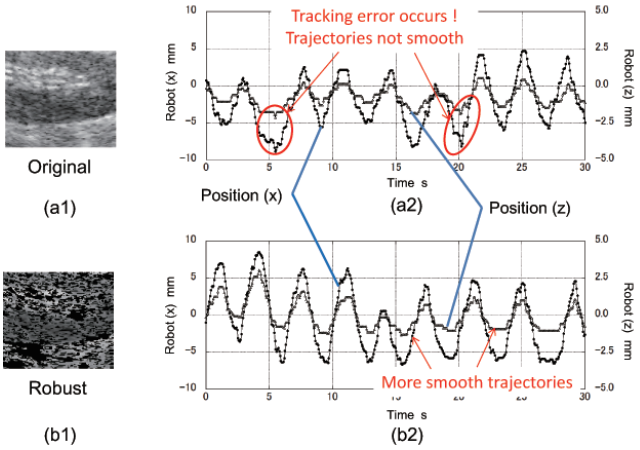

Fig. 10. Experimental results of realtime tracking and following experiment.

system in the x direction, and the value of 3D positioning sensor [28] in the y direction in order to enhance the robustness of tracking and following the affected area.

In Fig. 11, the fact that the correlation value is highly maintained shows that the IQ, which is illustrated in Section II-F, of the ultrasound images during tracking and following the target kidney could be preserved by the proposed novel robust template matching method and the constructed bed-type NIUTS.

In this experimsent, we applied a techinique to resume tracking status automatically by utilizing the acquired templates and 3D positioning sensor data. We will report the specification of this technique in the next report.

Specifically, Fig.11 shows that we can find the target kidney again properly and resume the tracking status in a few minutes, when the patient moves in the horizontal y-axis direction of the bed, we miss the tracking target kidney, and the normalized correlation value declines remarkably.

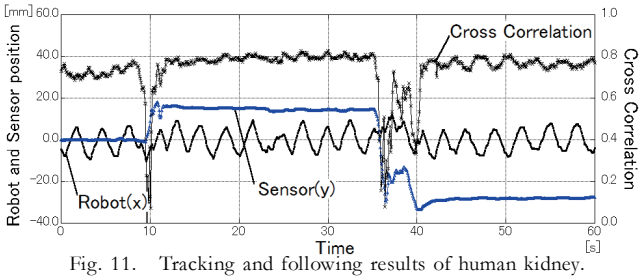

Fig. 11. Tracking and following results of human kidney.

V. CONCLUSIONS

In this paper, we proposed a novel robust template matching method to track and follow the target area to be treated. To confirm the effectiveness of the proposed robust template matching method, we conducted (i) offline tracking experiments and (ii) realtime online tracking and following experiments of the real human kidney in a healthy subject.

Our results confirmed that the proposed template matching method is more effective when only smaller templates are available. The average tracking miss rate by the proposed method could be reduced to be approximately one third of the conventional one.

The proposed novel robust template matching method could be applied to a motion tracking of the real human kidney based on the ultrasound images, which is the first successful report as far as I know. This robust visual servoing method have a great potential to give us a great tool to treat the tumors and stones precisely and safely.

VI. ACKNOWLEDGMENTS

This study was supported by Mr. Shin'ichi Tanaka, Mr. Takayuki Osa, Dr. Kanako Harada, Mr. Akira Sasaki, Prof. Shu Takagi (The Univ. of Tokyo), Mr. Manabu Watanabe, Mr. Toshiyuki Asano (Niigata Corporation), Mr. Takuji Osaka, Mr. Ryuichi Shinomura, Mr. Tsuyoshi Mitake, Mr. Takanori Itani (Hitachi Aloka Medical Corporation) the Translational Systems Biology and Medicine Initiative (TSBMI) and by the Global Center of Excellence for Mechanical Systems Innovation (GMSI) through the Japan Society for the Promotion of Science (JSPS) and the Ministry of Education, Culture, Sports, Science, and Technology of Japan.

REFERENCES

[1] P. I. Corke, S. Hutchinson, and G. D. Hager, *A tutorial on visual servo control*, in IEEE Transactions on Robotics and Automation, vol.12, pp.651-670, 1996.

[2] G. D. Hager and P. N. Belhumeur, *Efficient region tracking with parametric models of geometry and illumination*, in IEEE Trans. on Pattern Analysis and Machine Intelligence, vol.20, pp.1025-1039, 1998.

[3] F. Chaumette, *Image Moments: A general and useful set of features for visual servoing*, in IEEE Trans. Robotics and Automation, vol. 20, pp. 713-723, 2004.

[4] F. Chaumette and S. Hutchinson, *Visual servo control. II. Advanced approaches [Tutorial]* , in IEEE Robotics and Automation Magazine, vol. 14, pp. 109-118, 2007.

[5] Y. Nakamura, H. Kishi, and H. Kawakami, *Heartbeat Synchronization for Robotic Cardiac Surgery*, in Proc. of the 2001 IEEE International Conference on Robotics and Automation, pp.2014-2019, 2001.

[6] R. Ginhoux, J. Gangloff, M. de Mathelin, L. Soler, M.M.A. Sanchez, and J. Marescaux, *Active filtering of physiological motion in robotized surgery using predictive control, model predictive control and an adaptice observer*, in IEEE Trans. Robotics, vol. 21, pp. 67-79, 2005.

[7] A. Schweikard, G. Glosser, M. Bodduluri, M. Murphy, and J. R. Adler, *Robotic motion compensation for respiratory movement during radiosurgery*, in J. Computer Aided Surgery, vol. 5, pp.2631-277, 2000.

[8] J. Tang, S. Dieterich, and K. Cleary, *Respiratory motion tracking of skin and liver in swine for CyberKnife motion compensation*, in Proc. SPIE Medical Imaging, vol. 5367, pp.729-734, 2004.

[9] C. Ozhasoglu, C. B. Saw, H. Chen, S. Burton, K.Komanduri, N. J.Yue, S. M.Huq, and D. E. Heron, *Synchrony - cyberknife respiratory compensation technology*, in Medical Dosimetry, vol. 33, pp.117-123, 2008.

[10] R. Li, X. Jia, J. H. Lewis, X. Gu, M. Folkerts, C. Men, and S. B. Jiang, *Real-time volumetric image reconstruction and 3D tumor localization based on a single x-ray projection image for lung cancer radiotherapy*, in Medical Physics Letter, vol.37, no.6, pp.2822-2826, 2010.

[11] P. Abolmaesumi, S. E. Salcudean, W. H. Zhu, M.Sirouspour, and S. DiMaio, *Image-guided control of a robot for medical ultrasound*, in IEEE Trans. Robotics and Automation, vol. 18, pp. 11-23, 2002.

[12] I. Mikic, S. Krucinski, and J. D. Thomas, *Segmentation and tracking in echocardiographic sequences: Active contours guided by optical flow estimates*, in IEEE Transactions on Medical Imaging, vol. 17, pp.274-284, 1998.

[13] A. Krupa, G. Fichtinger, and G. Hager, *Real-time motion stabilization with B-mode ultrasound image speckle information and visual servoing*, in International Journal of Robotics Research, vol. 28, pp. 1334-1354, 2009.

[14] Y. Aoki, K. Kaneko, T. Sakai, and K. Masuda, *A study of scanning the ultrasound probe on body surface and construction of visual servo system based on echogram*, Journal of Robotics and Mechatronics, Vol.22, No.3, pp.273-279, 2010

[15] http://www.dornier.com/

[16] T. Ikeda, S. Yoshizawa, M. Tosaki, J. S. Allen, S. Takagi, N. Ohta, T. Kitamura, and Y. Matsumoto, *Cloud Cavitation Control for Lithotripsy Using High Intensity Focused Ultrasound*, in Ultrasound Med Biol, vol.32, no.9, pp.1383-1397, 2006.

[17] http://www.haifu-hifu.co.uk/

[18] http://www.insightec.com/

[19] F. Wu, Z.L. Wang, Z. Zhang, et al., *Acute biological effects of high-intensity focused ultrasound on H22 liver tumours in vivo*, in Chin. Ultrasound Med., vol.13, no.3, 1997.

[20] G. Tu, T.Y. Qiao, S. He, *An experimental study on high-intensity focused ultrasound in the treatment of VX-2 rabbit kidney tumours*, in Chin. J. Urol., vol.20, no.8, 1999.

[21] F. Wu, W.Z. Chen, J. Bai, J.Z. Zou, Z.L. Wang, H. Zhu, Z.B. Wang, *Pathological changes in malignant carcinoma treated with high-intensity focused ultrasound*, in Ultrasound Med. Biol. vol.27, no.8, pp.1099-1106, 2001.

[22] J.E. Kennedy, et al., *High-intensity focused ultrasound for the treatment of liver tumours*, in Ultrasound Med. Biol. vol.42, pp.931-935, 2004.

[23] N. Koizumi, J. Seo, T. Funamoto, A. Nomiya, A. Ishikawa, K. Yoshinaka, N. Sugita, Y. Homma, Y. Matsumoto, and M. Mitsuishi, "Technologizing and Digitalizing Medical Professional Skills for a Non-Invasive Ultrasound Theragnostic System," *in Journal of Robotics and Mechatronics*, vol.24, no.2, pp.379-388, 2012.

[24] N.Koizumi, S.Warisawa, M.Nagoshi, H.Hashizume, and M.Mitsuishi, "Construction methodology for a remote ultrasound diagnostic system," *in IEEE Trans. on Robotics*, vol. 25, 2009, pp 522-538.

[25] N. Koizumi, J. Seo, D. Lee, T.Funamoto, A.Nomiya, K.Yoshinaka, N.Sugita, H.Homma, Y.Matsumoto, and M. Mitsuishi, *Robust kidney stone tracking for a non-invasive ultrasound theragnostic system-Servoing performance and safety enhancement-, in Proc. of the 2011 IEEE International Conference on Robotics and Automation*, pp.2443-2450, 2011.

[26] N. Koizumi, J. Seo, Y. Suzuki, D. Lee, Kohei Ota, A.Nomiya, S.Yoshizawa, K.Yoshinaka, N.Sugita, H.Homma, Y.Matsumoto, and M. Mitsuishi, *A control framework for the non-invasive ultrasound theragnostic system, in Proc. of 2009 IEEE/RSJ Int. Conf. Intelligent Robotics and Systems*, pp.4511-4516, 2009.

[27] http://www.jastro.or.jp/guideline/

[28] http://www.ascension-tech.com/realtime/rttrakstar.php